

## The Deep Space Atomic Clock Mission

**Todd A. Ely<sup>(1)</sup>, Timothy Koch<sup>(2)</sup>, Da Kuang<sup>(3)</sup>, Karen Lee<sup>(4)</sup>, David Murphy<sup>(5)</sup>, John Prestage<sup>(6)</sup>, Robert Tjoelker<sup>(7)</sup>, Jill Seubert<sup>(8)</sup>**

<sup>(1)</sup>*Jet Propulsion Laboratory, California Institute of Technology, MS 301-121, 4800 Oak Grove Drive, Pasadena, CA 91109, 818-393-1744, [Todd.A.Ely@jpl.nasa.gov](mailto:Todd.A.Ely@jpl.nasa.gov)*

<sup>(2)</sup>*Jet Propulsion Laboratory, California Institute of Technology, MS 251, 4800 Oak Grove Drive, Pasadena, CA 91109, 818-354-8469, [Timothy.C.Koch@jpl.nasa.gov](mailto:Timothy.C.Koch@jpl.nasa.gov)*

<sup>(3)</sup>*Jet Propulsion Laboratory, California Institute of Technology, MS 238-600, 4800 Oak Grove Drive, Pasadena, CA 91109, 818-354-8332, [dakuang@jpl.nasa.gov](mailto:dakuang@jpl.nasa.gov)*

<sup>(4)</sup>*Jet Propulsion Laboratory, California Institute of Technology, MS 251, 4800 Oak Grove Drive, Pasadena, CA 91109, 818-354-3863, [Karen.Lee@jpl.nasa.gov](mailto:Karen.Lee@jpl.nasa.gov)*

<sup>(5)</sup>*Jet Propulsion Laboratory, California Institute of Technology, MS 238-600, 4800 Oak Grove Drive, Pasadena, CA 91109, 818-354-0845, [dwm@jpl.nasa.gov](mailto:dwm@jpl.nasa.gov)*

<sup>(6)</sup>*Jet Propulsion Laboratory, California Institute of Technology, MS 298, 4800 Oak Grove Drive, Pasadena, CA 91109, 818-354-3515, [John.D.Prestage@jpl.nasa.gov](mailto:John.D.Prestage@jpl.nasa.gov)*

<sup>(7)</sup>*Jet Propulsion Laboratory, California Institute of Technology, MS 298, 4800 Oak Grove Drive, Pasadena, CA 91109, 818-354-1873, [Robert.L.Tjoelker@jpl.nasa.gov](mailto:Robert.L.Tjoelker@jpl.nasa.gov)*

<sup>(8)</sup>*Jet Propulsion Laboratory, California Institute of Technology, MS 301-121, 4800 Oak Grove Drive, Pasadena, CA 91109, 818-354-4076, [Jill.Tombasco@jpl.nasa.gov](mailto:Jill.Tombasco@jpl.nasa.gov)*

**Abstract:** The Deep Space Atomic Clock (DSAC) mission will demonstrate the space flight performance of a small, low-mass, high-stability mercury-ion atomic clock with long term stability and accuracy on par with that of the Deep Space Network. The timing stability introduced by DSAC allows for a 1-Way radiometric tracking paradigm for deep space navigation, with benefits including increased tracking via utilization of the DSN's Multiple Spacecraft Per Aperture (MSPA) capability and full ground station-spacecraft view periods, more accurate radio occultation signals, decreased single-frequency measurement noise, and the possibility for fully autonomous on-board navigation. Specific examples of navigation and radio science benefits to deep space missions are highlighted through simulations of Mars orbiter and Europa flyby missions. Additionally, this paper provides an overview of the mercury-ion trap technology behind DSAC, details of and options for the upcoming 2015/2016 space demonstration, and expected on-orbit clock performance.

**Keywords:** navigation, atomic clocks, radiometric tracking, autonomy.

## 1. Introduction

The Deep Space Atomic Clock (DSAC) project plans to develop a small, low-mass atomic clock based on mercury-ion trap technology and demonstrate it in space, providing the unprecedented accuracy and stability needed for the next-generation deep space navigation and radio science.

Ground-based atomic clocks are the cornerstone of spacecraft navigation for most deep space missions because of their use in forming precision 2-Way coherent Doppler and range measurements. DSAC will provide an equivalent capability on-board a spacecraft for forming precision 1-Way radiometric tracking data (i.e., range, Doppler, and phase). With an Allan Deviation (AD) at 1 day of better than 2.E-14, DSAC will have a long term accuracy and stability that is equivalent to the existing Deep Space Network (DSN). Indeed, an early laboratory version of DSAC has demonstrated an AD < 1.E-15 @ 1 day. By virtually eliminating spacecraft clock errors from this data, DSAC enables a shift to a more efficient, flexible, and extensible 1-Way navigation architecture.

This paper presents a brief overview of DSAC's benefits to radio navigation and science, the technological innovations in DSAC, and options available to the project for demonstrating DSAC in space.

## 2. Benefits of the Clock to Navigation and Science

In today's 2-Way navigation architecture, the Earth ground network tracks a user spacecraft and then a ground-based team performs navigation. Relative to this, a 1-Way navigation architecture can deliver more data with better accuracy, and is enabling for future autonomous radio navigation. Some specific examples of how a 1-Way deep space tracking architecture can benefit NASA include:

1. The DSN can support multiple downlinks on a single antenna, called Multiple Spacecraft Per Aperture (MSPA). Since DSAC enabled 1-Way radiometric tracking doesn't require an uplink it can take full advantage of MSPA. For instance, at Mars two spacecraft equipped with DSAC can be tracked simultaneously on the downlink by a single antenna, while, with the current 2-Way tracking capability, those two spacecraft must split their time on the uplink. An example of the benefits to Mars orbit determination is provided next in Section 2.1.
2. Deep space users with DSAC can utilize full view periods for tracking, unlike 2-Way tracking, which reduces the available tracking time of the view period by the round trip light time. As an example, Cassini's Northern hemisphere view periods at Goldstone and Madrid are on the order of 11 hrs, so a round trip light time in the 4 – 5 hr range yields an effective ~ 6 hr 2-Way pass. A 1-Way pass using DSAC can utilize the full view period of 11 hrs, a near *doubling* of the usable data without needing to transition into a complicated 3-Way tracking operation across multiple ground stations.
3. For outer planet missions, solar corona plasma effects are a frequency-dependent error source that dominates over other measurement errors and affects radiometric tracking across both short and long time scales. Use of a Ka-only 1-Way downlink reduces these effects by 10 times relative to the typical user on an X-up/Ka-down 2-Way paradigm. Indeed the Europa Flyby Mission's gravity science results needed for determining the presence of an ocean underneath the crustal ice requires Ka-band tracking, which is

enabled via having DSAC. This example has been studied by the DSAC team with preliminary results provided in Section 2.2.

4. Planetary atmosphere investigations using radio occultations can benefit from DSAC as well. Compared to today's radio occultations that rely on 1-Way tracking derived using ultra stable oscillators, DSAC enabled measurements are upwards of 10 times more accurate on the time scales relevant to these experiments (that is, the several minutes that a spacecraft radio signal to Earth rises and sets as it passes through the atmosphere of interest before being occulted by the planet).
5. A 1-Way uplink received by a DSAC-enabled spacecraft with a properly configured and capable on-board navigation system is able to self-navigate in deep space. Autonomous deep space navigation has been demonstrated using optical navigation with the Deep Space 1 (DS1) and Deep Impact missions [1], [2]. However, a complete implementation of a fully autonomous on-board navigation system would couple a DSAC-enabled 1-Way forward radiometric tracking system with optical tracking from a camera system [5]. This would combine the strengths of radio navigation for determining absolute location in deep space and in planetary orbit with the target relative navigation provided by the optical system. A combined 1-Way radiometric and optical autonomous navigation system would provide a powerful solution for robotic missions where ground-in-the-loop operations are impossible (deep space encounters, planetary capture, real-time orbital operations, etc.), as well as supporting human exploration missions beyond low Earth orbit that require crewed operations without ground support. An example of this benefit is explored for a Mars robotic lander in Section 2.3

## 2.1. Mars Orbit Determination Example

At this time, deep space Doppler navigation depends primarily on 2-Way signals, as current onboard oscillators exhibit large frequency drifts unsuitable for navigation in which long gaps exist between tracking passes. However, the frequency stability performance of DSAC implies that future navigation may rely on 1-Way tracking data as the clock drift is essentially removed. A simulation study comparing the estimated solution quality given 2-Way Doppler data and DSAC-enabled 1-Way Doppler data was conducted for an orbiter in a near-polar sun-synchronous orbit configuration similar to that of the Mars Reconnaissance Orbiter. The estimation analysis framework simulated orbit reconstruction performed as part of standard spacecraft operations.

Sixty-second X-band 2-Way and 1-Way Doppler measurements were generated from a nominal trajectory and degraded with Gaussian noise ( $N[0, 0.00229 \text{ Hz}]$ ). The 1-Way Doppler measurements were further degraded with white frequency noise in accordance with the DSAC performance (1e-14 at 1 day). Realistic tracking schedules were derived for both 1-Way and 2-Way tracking. While the 2-Way tracking has long duration gaps due to shared antennae time, the 1-Way tracking takes advantage of MSPA to produce continuous (minus Earth occultation) tracking data (Figure 1).

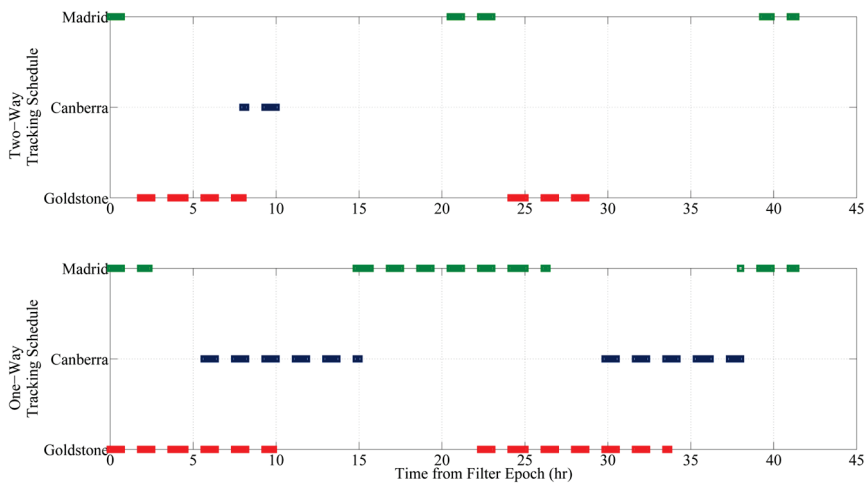


**Figure 1:** Simulated DSN tracking schedule for Mars orbiter example.

modeled as white noise processes; the drag scale factor was estimated at periareion and the frequency offset was estimated at each measurement time. The *a priori* uncorrelated uncertainties were 100 km for each position component, 0.01 km/sec for each velocity component, 10% and 20% of the nominal solar pressure and drag scale factors, respectively, and 1e-9 for  $J_{12}$  and  $J_{13}$ . The frequency bias uncertainty was 3 mHz to account for the DSAC clock performance at a 60-second count time.

In general, the 1-Way solution outperforms the 2-Way solution for each of the estimated parameters. As presented in Figure 2, the 1-Way position solution uncertainty is approximately 3 to 5 times smaller than that of the 2-Way solution during tracking periods. The 2-Way radial and transverse position uncertainty inflation over hours 10 through 20 and 30 through 40 corresponds to gaps in the tracking data; the relative uncertainty increases by an order of magnitude over the data gaps, largely due to the lack of atmospheric drag information. These results provide a metric for the navigation that can be achieved given onboard oscillator stability at the performance level of DSAC, and demonstrate the feasibility of a 1-Way Doppler tracking architecture for a Mars orbiter. The strength of MSPA is manifested as an increase in orbit knowledge when tracking is not interrupted, and in

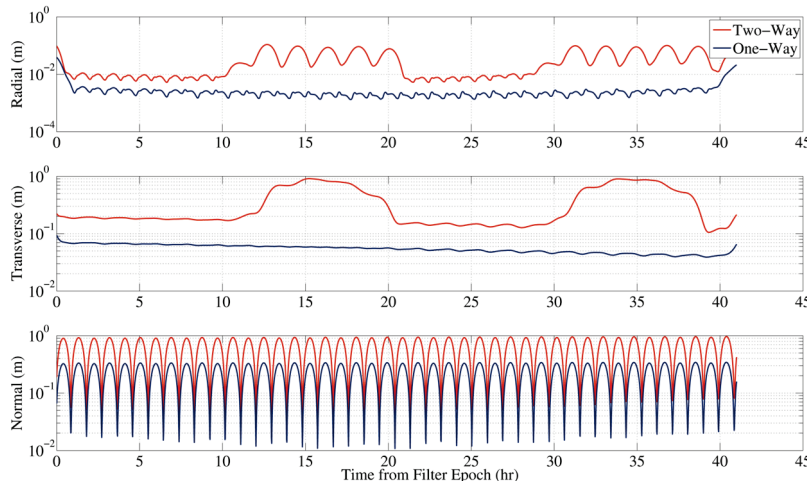


**Figure 2:** Comparison of estimated position uncertainty ( $1\sigma$ ) for 2-Way and 1-way Doppler tracking.

A sequential Kalman filter estimated the spacecraft's inertial position and velocity relative to Mars, a constant solar pressure scale factor, a stochastic atmospheric drag scale factor, and the Martian zonal gravity terms  $J_{12}$  and  $J_{13}$ . A stochastic signal frequency offset was also estimated for the 1-Way tracking scenario. Both stochastic parameters were

particular provides more complete recovery of the stochastic dynamics.

## 2.2. Europa Flyby Mission Gravity Science Example

Several proposed and selected missions are slated to further explore the Jovian system, with Europa of notable interest due to the potential of a subsurface liquid water ocean. A definitive answer regarding the existence of a subsurface ocean may be answered via estimation of Europa's gravitational tide. For a Europa flyby mission it is desirable to reduce the second-order, second-degree Love number ( $k_{22}$ ) uncertainty below 0.05. The proposed mission used as a baseline for this assessment of DSAC performance accumulates tidal information via a series of 34 low-altitude Europa flybys performed from February 2029 through August 2030 [3].

It was assumed that continuous radiometric tracking is available for a four-hour window centered on the close approach of each flyby. Sixty-second 2-Way Doppler measurements were simulated on X-band (8.4 GHz) and Ka-band (32.0 GHz) and degraded with Gaussian measurement noise (0.1 mm/sec for X-band and 0.01 mm/sec for Ka-band). 1-Way Ka-band measurements were also generated and degraded with system noise and DSAC clock noise. Currently, only the Goldstone DSN complex is capable of Ka-band 2-Way tracking; while Canberra and Madrid can support a Ka-band downlink, these complexes can only support X-band on the uplink. Moving to a 1-Way downlink tracking paradigm removes the uplink frequency constraint, enhancing the tracking data quality by an order of magnitude. Furthermore, any suitable antenna outfitted with a Ka-band receiver can track the downlink signal, resulting in the possibility of increased ground coverage and receiver robustness as a contingency for receiver downtime and weather outages.

Several parameters were estimated during each flyby: the inertial spacecraft position and velocity relative to Europa (*a priori*  $\sigma = 100$  km and 0.01 km/sec), three constant accelerations ( $\sigma = 5\text{e-}11$  km/sec<sup>2</sup>), Europa's gravitational parameter ( $\sigma = 10\%$  of nominal value), Europa's second-order Love numbers ( $\sigma = 0.2$ ), and a 20 x 20 Europa gravity field ( $\sigma$  derived from Kaula's rule).[3] A stochastic frequency bias parameter was estimated for the 1-way tracking scenario ( $\sigma = 1.21$  mHz). To accumulate the Europa gravity information, the global portion of the *a priori* covariance for a given flyby was defined to be the global portion of the *a posteriori* covariance of the previous flyby. The position, velocity and acceleration *a priori* covariance values were assigned as the uncorrelated values defined above.

In order to demonstrate the significance of the selected 2-Way or 1-Way tracking architecture on gravitational tide estimation, several possible scenarios were analyzed. Figure 3 presents the estimated  $k_{22}$  uncertainty for each scenario. As expected given the higher measurement quality, Ka-band tracking allows the gravity parameter to be recovered better than X-band tracking. The gravity science objective ( $\sigma_{k_{22}} \leq 0.05$ ) cannot be achieved with 2-Way Doppler tracking at X-band. Taking advantage of Ka-band tracking at Goldstone allows for the objective to be met after 28 flybys, while implementing Ka-band tracking at all DSN complexes decreases the number of required flybys to 12. DSAC 1-Way Ka-band tracking allows the  $k_{22}$  parameter to be recovered to less than 0.05 in 12 flybys, a 57% reduction in required flybys compared to the best 2-Way performance given current DSN capabilities. Processing all flybys reduces the final  $k_{22}$  uncertainty to 0.020 for the 1-Way case, whereas the Ka-/X-band 2-Way case reduces the uncertainty to 0.040. The results show that utilizing DSAC-enabled 1-Way Doppler tracking improves the overall gravitational tide science return by 50% compared to the best 2-Way tracking scenario currently available. Additionally, relying on DSAC 1-Way radiometric data to

achieve the gravity goal reduces mission risk by decreasing the number of flybys required to meet the minimum science objective.

### 2.3. Autonomous Navigation and Mars Entry Example

Given that DSAC-based 1-Way radiometric data is as accurate or better, in many cases, than its 2-Way counterpart, it enables a shift towards autonomous radio navigation where the tracking data is collected on the uplink (or forward link) and processed on-board. In the current ground processing paradigm, the timeliest trajectory solutions that are available on-board are stale by several hours to account for light time delays and ground navigation processing time. Real time trajectory solutions are enabled via on-board 1-Way radio tracking using DSAC coupled with an autonomous GNC capability that processes this data. Such a capability can significantly enhance real time GNC events such as entry, descent, and landing; orbit insertion; flyby; or aerobraking via improving the trajectory knowledge necessary to execute these events robustly, efficiently, and in some cases with more accuracy.

As a specific example, delivery of a Mars lander to the top of the atmosphere (i.e., entry) using current ground based navigation procedures typically yields a knowledge uncertainty of 2 – 3 km

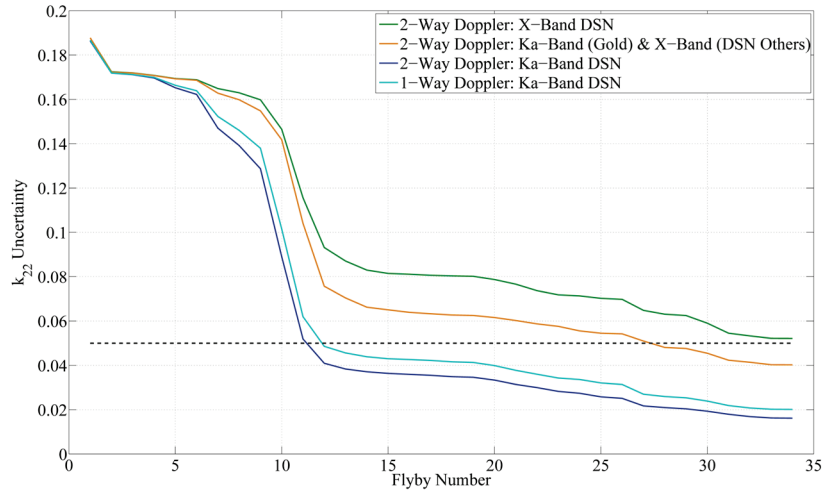


**Figure 3:**  $k_{22}$  estimated uncertainty for selected tracking architectures.

(3 sigma), which results from uploading a final trajectory solution upwards of 6 hours prior to entry [4]. With DSAC 1-Way radio-tracking on the uplink and an onboard GNC system this knowledge uncertainty reduces to a handful of meters because the tracking and associated trajectory solution are available continuously and nearly instantaneously, including during entry [4]. This trajectory solution coupled with active guidance during the lander’s hypersonic descent phase can effectively ‘fly-out’ any residual top of the atmosphere delivery error to get the lander back on its nominal descent trajectory prior to parachute deployment. A 2006 study lead by Wolf [5] on pinpoint landing (i.e., < 100 m landing error) trades showed that reducing the delivery error to the parachute deployment would result in  $\sim 100$  kg propellant savings for a MSL-size pin-point lander in moderate winds. By essentially eliminating the effects of atmosphere delivery errors, the powered descent portion of a pin-point landing need only correct for wind drifts and map tie error, thus reducing the overall delta V required. Use of DSAC for entry is an important step towards achieving an efficient (resource friendly) pin-point landing.

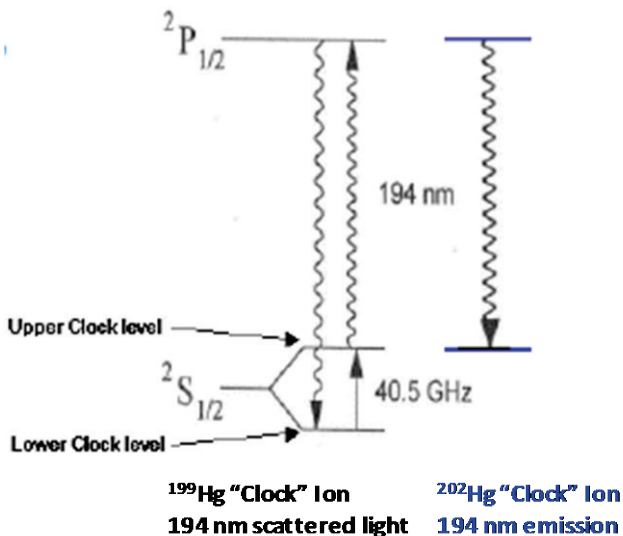


**Figure 4:** Mercury ion clock transition and UV transition for state selection/detection.

### 3. Mercury Ion Trap Technology and Application to DSAC

Mercury ion clocks based on the ground state hyperfine transition in trapped  $^{199}\text{Hg}$  ions are a promising technology for an operational space clock that simultaneously addresses reliability, size, weight and power (SWaP), and stability performance requirements. Trapped ions are easy to handle in a microgravity environment, and the 40.5 GHz hyperfine transition (Figure 4) is the highest frequency and least magnetically sensitive of the alkali-like atoms and ions that have been investigated for atomic clock applications. Room temperature, lamp-based mercury quadrupole and multi-pole linear ion trap based frequency standards have been highly developed for ground applications

resulting in three generations of reliable and continuously operating mercury ion frequency standards with good accuracy and very high stability [6-11]. Multi-pole [8] and compensated multi-pole ion traps [10] have proved to effectively eliminate residual ion number sensitivity, resulting in UTC-level timescale demonstration with a single mercury ion trap standard having long term frequency variation at the low  $10^{-17}$  level per day [9,11]. NASA technology efforts continued small ion trap development [12] and very long ion trap lifetimes have been obtained in a getter pumped vacuum assembly designed to be baked to 450 °C and stable signal-to-noise has been demonstrated over several years [13]. Long term stability and environmental sensitivity in this high temperature bake-out ion trap assembly has yet to be characterized, though operation with only a sealed getter pump evacuating a larger multi-pole ion trap assembly baked to 200 °C has demonstrated very stable clock operation over 9 months [14]. These continued NASA/JPL advances in ultra-stable timekeeping and small ion trap “vacuum tube” technology have positioned the mercury ion technology to be realized as a spacecraft-based navigation-capable mercury ion frequency standard.

Mercury ion clocks developed at JPL are passive frequency standards (Figure 5): the ions are used to steer the local oscillator (LO). The stability of the frequency output of the clock for time intervals less than one day is highly dependent on the quality of the LO. The optimum stability performance of the ion clock for time intervals less than  $\sim 10,000$  seconds is inversely proportional to  $\text{SNR} * Q * \tau^{1/2}$  (where SNR is the achieved Signal-to-Noise Ratio in a 1 Hz bandwidth for a single interrogation, Q is the atomic line resolution, and  $\tau$  is the averaging interval). Since Q is inversely proportional to the clock transition interrogation time, short term LO stability limits the practical clock interrogation cycle for a specific implementation. In the laboratory there exist several LO options such as a cryogenic oscillator or hydrogen maser, but for spaceflight we are currently restricted to using a quartz-based LO. The first mercury ion clock implemented at JPL was able to control all three LO's with mercury ions confined in a quadrupole ion trap assembly [7] with the performance dependent on the LO implementation.

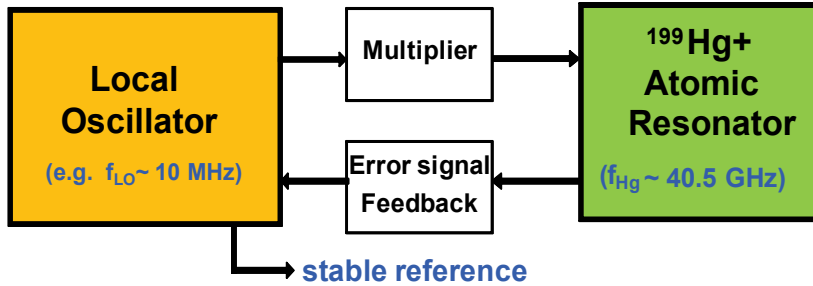


**Figure 5:** Mercury ion clock disciplining a Local Oscillator.

While the ion cloud size in the quadrupole ion trap was small ( $\sim 2$  mm diameter by  $\sim 7$  cm long), the surrounding vacuum/optics/magnetic system was built with larger vacuum system, optics, and electronic components. The entire ion clock required 2 racks of space and more than 1 kW of power. Four of these standards disciplining quartz LO's were developed and several years of operational experience were obtained in JPL's Frequency Standards Test Laboratory and at remote sites in NASA's Deep Space Network.

A space ion clock for deep space navigation and/or GNSS applications [15] should consume little power (< 20 W for deep space operations and < 30 W for GNSS), fit in a volume of a few liters, have simplified external interfaces, and be very reliable. A prototype small ion clock technology for potential application in deep space has been under development at JPL for some time. Figure 6 shows a hardened ion trap/vacuum tube assembly recently assembled at JPL. A version of this trap has been operated in the lab demonstrating an AD at 1 day near  $1.0 \times 10^{-15}$  as shown in Figure 7. For comparison, the performance of current state of the art USOs and Rubidium (Rb) atomic standards are also shown in the figure. This successful laboratory demonstration was a key element that paved the way for the DSAC project being selected as a NASA Technology Demonstration Mission in Aug 2011.

#### 4. Mission Overview

The DSAC mission is planning a space flight demonstration in 2015/2016 that will prove the clock's functionality and suitability for a variety of future space missions. A successful conclusion of the mission's space operation will bring DSAC to a NASA Technology Readiness Level (TRL) of 7 from its present day level of 5. In other words, DSAC will be an advanced prototype of a mercury ion space clock that, with minimal additional investment and minimal risk, can be engineered into an infusion-ready flight instrument. In addition to validating the clock's performance in an operational space environment (thermal, vacuum, vibration, magnetic,



**Figure 6:** Ion trap/ vacuum tube assembly engineered following space vacuum tube design principles and bakeable to  $450^{\circ}\text{C}$ .

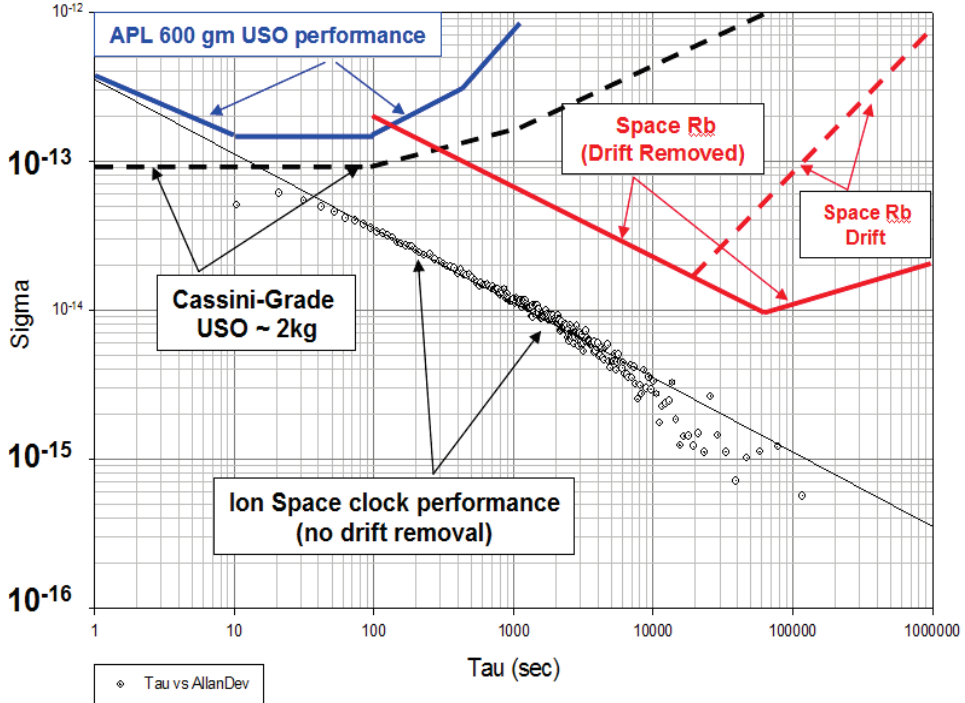


**Figure 7:** Measured (frequency domain) clock stability (Allan Deviation) of a sealed tube prototype  $^{199}\text{Hg}$  ion clock. A typical GPS Rubidium space clock (red) and USO (blue and black dash) is shown. The Ion Clock data shows no significant frequency drift.

radiation, and zero-g), the on-orbit experiment will validate DSAC as a viable navigation instrument in a system end-to-end navigation demonstration. Presently, the DSAC project has two pathways towards conducting a space-flight experiment: the first as a hosted payload on a Low Earth Orbit (LEO) spacecraft that uses GPS radiometric tracking to perform orbit and clock determination; the other as a navigation experiment using the Deep Space Network (DSN) on NASA’s InSight mission, recently selected by NASA’s Discovery Program. Each of these options will be described in more detail.

#### 4.1. Low Earth Orbit Demonstration Option

##### 4.1.1. Mission and Payload Description

A demonstration of the technology from LEO is facilitated by the use of GPS. In this environment, the DSAC payload (DSAC-P) comprises three main assemblies: the Ion Clock, an Ultra-Stable Oscillator (USO), and a GPS receiver and antenna. The three assemblies all fit within the payload bay of a standard ESPA-compatible small satellite, such as a Surrey Satellite Technology SSTL-150 (the current leading candidate hot spacecraft for a LEO demonstration), and the antenna, a standard Sensor Systems model with a choke ring for multipath suppression, is situated to view GPS satellites in the zenith-facing hemisphere. An illustration of a candidate payload configuration is shown in Figure 8. The demonstration model measures less than 30 cm by 22 cm by 18 cm, with a mass of less than 12 kg, and DC power consumption less than 48 W. The Ion Clock is powered from the host spacecraft’s 28-volt power bus, transmits its health and status telemetry to the host to be downlinked to the ground, and delivers the stable 10 MHz signal to the GPS receiver. The USO serves as the local oscillator for the Ion Clock. The USO is an ovenized crystal oscillator with a short-term stability of less than  $3 \times 10^{-13}$  and a frequency drift

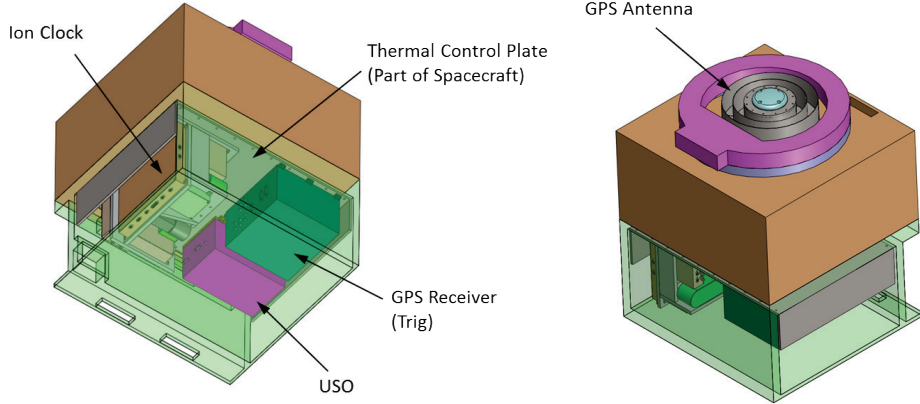


**Figure 8:** Candidate payload configuration on a LEO spacecraft.

of less than  $10^{-10}$  in a day. The Ion Clock provides an external reference input to the GPS receiver. The GPS receiver collects L1-band and L2-band carrier phase and pseudorange data from all satellites in view of the GPS antenna. The GPS receiver starts collecting data after booting up without any commanding. The GPS data is transferred in Blackjack packets (e.g. packets containing fields such as timestamps, pseudo-range, phase) via an RS-422 connection to the host spacecraft for transmission to the ground which are then processed to determine both orbit and clock performance with a mission requirement to validate the clock's combined stability and drift at 1 day to have an AD of  $< 2.E-14$ .

#### 4.1.2. Preliminary Investigation Performance

Using the JPL GIPSY-OASIS software, extensive simulations regarding the performance of DSAC as a secondary payload on-board a LEO spacecraft based on SSTL-150 have been performed. The key spacecraft assumptions used in the simulations are as follows:

- Total mass = 180 kg
- Solar panels lie perpendicular to zenith in order to minimize multi-path effects
- Total solar panel area =  $2.4 \text{ m}^2$
- Bus dimensions: 24" wide x 28" deep x 35.9" length
- Zenith-pointing GPS antenna for DSAC payload
- Sun-synchronous circular orbit with the ascending node at 1:30 pm local time
- Orbit height: 300 to 700 km with a nominal height of 600 km

The GIPSY-OASIS software is used extensively for the determination of the GPS constellation orbit and clocks and precise orbit determination (POD) for LEO spacecraft such as gravity missions (e.g., CHAMP and GRACE) and the altimetry missions (e.g., TOPEX/Poseidon, Jason-1, Jason-2/OSTM). This software is also used by the geodetic community to determine the precise location of hundreds of ground GPS sites. Several features of GIPSY-OASIS make it the software of choice to study the performance of the DSAC clock in space, among them:

- Unlike other POD software packages it does not eliminate the receiver clock error using the single difference technique. It is this receiver clock error  $x(t)$  (see below for its definition) that is used to determine the DSAC clock stability.

- The software that is used to simulate and analyze the data has been operationally tested.

The phase (in cycles) of a perfect clock is given by

$$\phi(t) = f_o t + \phi_0 \quad (0)$$

where  $f_o$  is its nominal output frequency (in Hz),  $t$  is the time (in seconds), and  $\phi_0$  is the initial phase. For any real imperfect clock, such as the DSAC clock, the phase is given formally as

$$\phi(t) = f_o(t + x(t)) + \phi_0 \quad (0)$$

where  $f_o x(t)$  is a measure of how the phase differs from a perfect clock. The aim of the GPS analysis for the DSAC mission is to determine how well the DSAC on-orbit investigation will be able to estimate  $x(t)$  in the presence of a realistic set of system errors. Estimates of the phase can then be used to determine the AD,  $\sigma_y(\tau)$ , which can be defined using

$$\sigma_y^2(\tau) = \frac{1}{2(N-2)\tau^2} \sum_{i=1}^{N-2} [x(t_i + 2\tau) - 2x(t_i + \tau) + x(t_i)]^2 \quad (0)$$

The AD provides a useful measure of the stochastic properties of the time series and ultimately a clock's stability. A variety of other measures can be used to determine the statistical properties; the results shown here use the Modified Allan Deviation (MAD). For more details on these statistical measures it is recommended that the reader consult Riley's 'Handbook of Frequency Stability Analysis' (NIST Special Publication 1065) [16]. In our simulations of the DSAC clock we model  $x(t)$  as a random walk (equivalent to white frequency noise) which leads to both the AD and MAD to decrease proportionally to  $1/\sqrt{\tau}$ . The real DSAC clock is expected to show this behavior as illustrated in Figure 7. For DSAC performance the AD (or MAD) at  $\tau = 1$  day is of primary importance because it is a key characteristic for use in deep space navigation that differentiates the clock from a USO.

Our typical simulation is conducted as follows:

- Select a start time and total time span of simulation (typically 5 days).
- Select data observation cadence (300s, typical for operational GPS analysis).
- Create the simulated truth orbit for the LEO spacecraft over the total time span using the spacecraft properties stated above subject to a variety of forces including gravity, drag, and solar pressure. No maneuvering is modeled at this point.
- Create simulated perfect ionosphere-free carrier phase and pseudo-range data (referred to as LC and PC data) with no errors at each observation cadence interval from those GPS satellites which are visible to the DSAC GPS receiver. For the truth data the GPS orbits and clocks are simulated using JPL's contribution to the final IGS data products, and the nominal GPS orbit and clock models used for the filter are generated using JPL's rapid data products. In this manner, realistic GPS errors can be injected into the simulation at levels that are consistent with current IGS performance (namely, 2 cm GPS orbit errors and 50 ps GPS clock errors).

- Add measurement noise and DSAC clock errors (injected as random walks in phase either with equivalent AD at 1 day of either 1.0E-15 or 1.0E-14) to the perfect LC and PC data to create the simulated truth data set to be analyzed for extracting  $x(t)$ .
- Analyze the combined LC and PC simulated data using the standard GIPSY precise point positioning (PPP) application software GD2P which includes estimating  $x(t)$  every 300s.
- Run two different Kalman filter models are to produce  $x(t)$  estimates :
  - Kinematic Model (KM) – position, velocity, and  $x(t)$  are estimated from essentially just the data (ignoring spacecraft dynamics).
  - Reduced Dynamic Model (RDM) – the most accurate spacecraft dynamical model is used but due to spacecraft force modeling errors it is necessary to estimate and use small stochastic accelerations along with the position, velocity, and  $x(t)$  to try to account for the spacecraft force modeling errors.
- Given a set of  $x(t)$ , compute the MAD for the full range of  $\tau$ -values given the 5-day simulation range (300s to beyond a day).

Initial results of the simulations characterize the impact of drag errors, a significant model error source for LEOs, on the ability to estimate DSAC's AD. The standard density model used by many POD groups around the world is DTM2000, which superseded the DTM94 model. To estimate the error in the DTM2000 density model we take the difference between it and the DTM94 density model as an indication of how well density can be modeled. The resulting difference in drag acceleration (for the given spacecraft model) has an RMS value of  $0.05 \text{ nms}^{-2}$  at 600 km and  $0.71 \text{ nms}^{-2}$  at 300 km. Thus, only a factor of 2 in height leads to a change by a factor of 140 in the drag acceleration. Furthermore these differences are not purely stochastic but exhibit a periodic behavior with periods that include both the orbital and half-orbital period. This error is injected by creating the truth orbit using the DTM2000 model, but the simulated data is analyzed using the DTM94 model. In order to correct for this a small acceleration along the velocity direction (which is the same as the along-track direction for a circular orbit) must be solved for. Figure 8 and Figure 9 show how the MAD varies with  $\tau$  for a DSAC clock with  $\sigma_y(1 \text{ day}) = 10^{-14}$  (project requirement) and  $\sigma_y(1 \text{ day}) = 10^{-15}$  (expected clock performance) at a 600 km orbit, respectively. In both cases, the overall project requirement for clock validation performance of  $\sigma_y(1 \text{ day}) = 2 \times 10^{-14}$  (including systematic errors of non-clock errors from the validation system) is easily met. In order to obtain the RDM results presented here care needs to be taken in choosing the input parameters used to model these small additional accelerations, otherwise worse performance is obtained. Also, the 4 simulations described here represent only a small fraction of those undertaken so far on the Surrey spacecraft (so far a total of 137). A variety of other issues have been studied and more will be studied as the various mission design trade-offs become clearer.

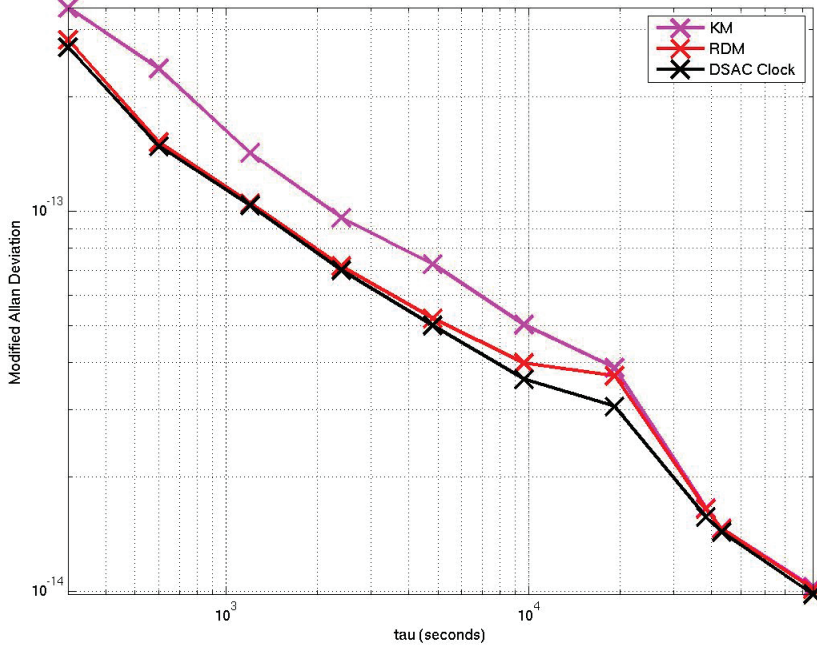


**Figure 9:** DSAC simulation result for a 600 km orbit. Plot of MAD versus  $\tau$  between 300 s and 1 day for KM (magenta), RDM (red), and input clock (black) with  $\sigma_y(1 \text{ day}) = 10^{-14}$  (project required clock performance). Note improvement of RDM over KM and that  $\sigma_y(1 \text{ day}) = 2 \times 10^{-14}$  (required clock validation) is easily met.

#### 4.2. Demonstrating on InSight

The addition of InSight as an option for demonstrating DSAC has only recently become available so the analysis and engineering of this option is in its preliminary stages. Initial thoughts on an InSight demonstration are that it will be during the cruise phase and require only modifications to the cruise stage. In particular, the DSAC payload on InSight would consist of the Ion Clock and associated USO that would tie into the currently manifested Small Deep Space Transponder (SDST) and InSight’s X-band antenna system. Other spacecraft accommodations from Insight include access via 1553 to Insight’s avionics to downlink the health and status telemetry of the clock, and 28-V power. With this system the standard 2-Way carrier phase data products that are measured at the DSN would be augmented with 1-Way carrier phase measurements derived from DSAC, also measured at the DSN. This would allow the DSAC investigation to perform end-to-end navigation experiments that would demonstrate DSAC-based 1-Way navigation relative to its 2-Way counterpart, and, if simultaneous 2-Way/1-Way measurements can be obtained, allow for in-space validation of the clock’s performance.

#### 5. Conclusion

The DSAC mission is on its way towards developing and operating a mercury ion trap clock in space that will demonstrate the stability necessary for forever changing the way NASA performs radio navigation and science. Indeed, if successful, DSAC will enable deep space 1-Way Doppler and ranging measurements that can be up to 10 times more accurate than their 2Way counterparts. The combination of this accuracy with the flexibility afforded by a 1-Way tracking

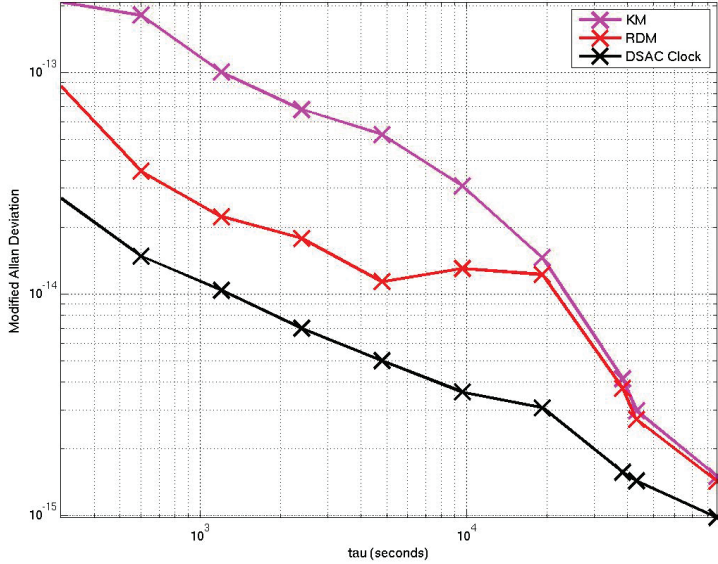


**Figure 10:** DSAC simulation result for a 600 km orbit. Plot of MAD versus  $\tau$  for KM (magenta), RDM (red), and the input clock (black) with  $\sigma_y(1 \text{ day}) = 10^{-15}$  (expected clock performance). Note large improvement of RDM over KM and that  $\sigma_y(1 \text{ day}) = 2 \times 10^{-14}$  project requirement is easily met.

architecture will improve overall tracking efficiencies as well as enable ways of operation not available today.

## 6. References

- [1] S. Bhaskaran, J. E. Riedel, B. M. Kennedy, and T. Wang, “Navigation of the Deep Space 1 Spacecraft at Borrelly,” *AIAA/AAS Astrodynamics Specialist Conference*. Monterey, CA, 2002.
- [2] D. G. Kubitschek, N. Mastrodemos, R. A. Werner, S. P. Synnott, S. Bhaskaran, J. E. Riedel, B. M. Kennedy, G. W. Null, and A. T. Vaughan, “The Challenges of Deep Impact Autonomous Navigation,” *Journal of Field Robotics*, vol. 24, no. 4, pp. 339–354, 2007.
- [3] R. S. Park, S. W. Asmar, B. B. Buffington, B. Bills, S. Campagnola, P. W. Chodas, W. M. Folkner, A. S. Konopliv, and A. E. Petropoulos, “Detecting tides and gravity at Europa from multiple close flybys,” *Geophysical Research Letters*, vol. 38, no. 24, Dec. 2011.
- [4] A. Wolf, “Pinpoint Landing Technology Assessment,” in *MSR Technology Workshop*, 2008, p. 20.
- [5] A. A. Wolf, J. Tooley, S. Ploen, M. Ivanov, B. Acikmese, and K. Gromov, “Performance Trades for Mars Pinpoint Landing,” in *2006 IEEE Aerospace Conference*, 2006, pp. 1–16.
- [6] J. D. Prestage, G. J. Dick, and L. Maleki, “New Ion Trap for Frequency Standard Applications”, J. Appl. Phys., 66, pp. 1013–1017, Aug. 1989.

- [7] R.L. Tjoelker, C. Bricker, W. Diener, R.L. Hamell, A. Kirk, P. Kuhnle, L. Maleki, J.D. Prestage, D. Santiago, D. Seidel, D.A. Stowers, R.L. Sydnor, T. Tucker, “*A Mercury Ion Frequency Standard Engineering Prototype for the NASA Deep Space Network*”, Proc. 50th IFCS, Honolulu, Hawaii, June 5-7, 1996.
- [8] J.D. Prestage, R.L. Tjoelker, L. Maleki, “*Higher Pole Linear Traps For Atomic Clock Applications*”; 13<sup>th</sup> European Frequency and Time Forum, Besancon, France, April 13-16, 1999.
- [9] R.L. Tjoelker, J.D. Prestage, P.A. Koppang, T.B. Swanson, “*Stability Measurements of a JPL Multi-pole Mercury Trapped Ion Frequency Standard at the USNO*” ; Proc. 2003 Joint EFTF and IEEE IFCS , Tampa, FL; May 5-8, 2003.
- [10] E.A. Burt and R.L. Tjoelker, “*Characterization and Reduction of Number Dependent Sensitivity in Multipole Linear Ion Trap Standards (LITS)*”; in Proc. of the 2005 Joint PTTI / IFCS, Vancouver, Canada; Aug 29-31, 2005.
- [11] E.A. Burt, W. Diener, and R. L. Tjoelker, ”*A Compensated Multi-pole Linear Ion Trap Mercury Frequency Standard for Ultra-Stable Timekeeping*”, IEEE TUFFC 55, 2586 (2008).
- [12] J.D. Prestage, M. Beach, S. Chung, R. Hamell, T. Le, L. Maleki, and R.L. Tjoelker, “*One Liter Ion Clock: New Capability for Spaceflight Applications*”; 35th PTTI, San Diego, Dec. 2003.
- [13] J. D. Prestage, S. Chung, L. Lim, A. Matevosian; “*Compact Microwave Mercury Ion Clock for Deep-Space Applications*”; Proc. of the 2007 Joint IEEE Frequency Control Symposium and European Frequency and Time Forum, Geneva, Switzerland, May 2007.
- [14] E.A. Burt and R. L. Tjoelker, ”Prospects for Ultra-Stable time keeping with sealed vacuum operation in Multi-pole Linear Ion Trap Standards ”, in Proc. of 39th PTTI; Long Beach, California; Nov 26-29, 2007.
- [15] R.L. Tjoelker, E.A. Burt, S. Chung, R.L. Hamell, J.D. Prestage, B. Tucker, P. Cash, R. Lutwak, “*Mercury Atomic Frequency Standard Development for Space Based Navigation and Timekeeping*”, in Proc. of 43rd PTTI; Long Beach California, Nov 2011.
- [16] W.J. Riley, “*Handbook of Frequency Stability Analysis*, ” *NIST Special Publication 1065*, National Institute of Standards and Technology, Boulder, Co, July 2008.